Observation of the Z-dependence of laser-plasma corona temperature in investigation of half-integer harmonic radiation

V. Yu. Bychenkov, A. A. Zozulya, Yu. S. Kas'yanov, A. V. Kilpio, and V. T. Tikhonchuk

P. N. Lebedev Physics Institute, USSR Academy of Sciences

(Submitted 17 July 1982)
Zh. Eksp. Teor. Fiz. **84**, 936–946 (March 1983)

Simultaneous spectral-temporal and polarization measurements were performed, for the first time ever, of the laser-plasma emission at the frequencies $\omega_0/2$ and $3\omega_0/2$ following irradiation of targets having different atomic numbers Z by the second harmonic of a neodymium laser ($\lambda_0 = 0.53\,\mu$m). The experimental results on the generation of half-integer harmonics are interpreted on the basis of theoretical premises concerning the physical processes that take place in the region of one-quarter the critical density. It is concluded from an analysis of the spectra of the harmonics that the electron temperature increases with increasing atomic number of target material. This conclusion agrees with theoretical predictions that follow from the theory of the anomalous transport due to the development of ion-sound turbulence.

PACS numbers: 52.25.Ps

1. Interest in the investigation of nonlinear processes in a laser plasma, in the vicinity of the region of the one-quarter density $n_c/4$, has recently increased anew. This is due primarily by recognition of the fact that the anomalous absorption in this region can lead to a considerable growth of the number of high-energy electrons,[1] a result highly undesirable for controlled thermonuclear fusion. The nonlinear processes in the region of the one-quarter critical density manifest themselves, in particular, in the electromagnetic emission from a laser plasma at half-integer harmonics of the pump wave. An experimental investigation of this radiaiton is of great interest, since it can yield information on the turbulence level in the $n_c/4$ region, as well as provide an estimate of such important laser-plasma parameters as the electron temperature, the rate of expansion, and the degree of inhomogeneity. In addition, it is of definite physical interest to cast light on the relative role of different nonlinear processes in the generation of radiation at half-integer harmonic frequencies and a comparison of the experimental data with the available theoretical results.

Up to now, the emission mainly investigated was at the $3\omega_0/2$ frequency (Refs. 2–8); the registration of the $\omega_0/2$ radiation is a more complicated experimental task in view of the lack, in the corresponding region of the spectrum, of sufficiently sensitive radiation receivers with good time resolution. The last statement pertains primarily to the plasma produced by neodymium ($\lambda_0 = 1.06\,\mu$m) and CO_2 ($\lambda_0 = 10.6\,\mu$m) laser radiation. For this region, there are few and fragmentary data on the generation of the $\omega_0/2$ harmonic.

Registration of the $\omega_0/2$ harmonic in a laser plasma was first reported in Ref. 3. It must be noted that owing to the low intensity of the $\omega_0/2$ harmonic the spectrum was recorded with a photomultiplier point-by-point using several laser flashes. An attempt in Ref. 4 to record radiation at the frequency $\omega_0/2$ was unsuccessful. Measurement of the coefficient of conversion of the fundamental radiation into the $\omega_0/2$ harmonic was recently made in Ref. 9. According to this reference it amounts to 10^{-6}–10^{-7}.

Substantial progress in the study of the $\omega_0/2$ harmonic generation was achieved recently by going to heating radiation of shorter wavelength. In Ref. 10, generation of the $\omega_0/2$ harmonic was observed when targets were irradiated by the second harmonic ($\lambda_0 = 0.53\,\mu$m) of a neodymium laser. Similar experiments at the third harmonic of a neodymium laser were performed in Ref. 11.

We present here the results of spectral-temporal and polarization measurements, performed for the first time ever, of simultaneous emission from a laser plasma at the frequencies $\omega_0/2$ and $3\omega_0/2$. New information was obtained on the nonlinear processes in the $n_c/4$ region and on the mechanism of half-integer harmonic generation. The reduction of the harmonic emission spectra indicates that the corona temperature rises with increasing atomic number of the target material, a result that can be attributed to the suppression of the thermal conductivity at the laser-energy fluxes used in the experiment.

2. The emission from a laser plasma at the half-integer harmonics $\omega_0/2$ and $3\omega_0/2$ is connected with two parametric instabilities: two-plasmon decay and stimulated Raman scattering (SRS), which occur in the region of one-quarter the critical density ($n_c/4$). Emission of the frequency $\omega_0/2$ should be strongly refracted and emerge from the plasma at small angles to the normal to the plasma surface, since the $n_c/4$ region is critical for this radiation.[12] The directivity pattern of the radiation at the frequency $3\omega_0/2$ should be more isotropic.[12]

Generation of half-integer harmonics should be most effective in the case when the waves excited at a maximum growth rate are precisely the Langmuir waves, which are next transformed into emission at the harmonic frequencies. A part is played in the generation of the harmonic only by Langmuir waves that propagate almost along the inhomogeneity direction (more accurately, those waves for which the component of the wave vector $k_\perp$ satisfies the condition $k_\perp \lesssim \omega_0/c$). The maximum of the growth rate of the two-plasmon instability is reached in the pump-wave polarization plane at angles 45° to the wave vector and to the polarization vector.[13]

 0038-5646/83/030544-06$04.00

The foregoing arguments served as the basis for choosing the direction in which the radiation at the frequencies $\omega_0/2$ and $3\omega_0/2$ were recorded and the angle at which the target was irradiated in the present experiment.

3. We used a single-frequency neodymium-glass laser setup.[14] To convert the infrared radiation and to obtain the second harmonic we used a type-I KDP crystal measuring $50\times50\times18$ mm. The coefficient of conversion into the second harmonic was $\sim35\%$. The principal parameters of the radiation at which the measurements were made were: output energy up to 10 J, pulse duration 5 nsec, radiation contrast $>10^5$, and the energy density of the flux to the target, averaged over the pulse duration, when focusing with an $f/6$ lens reached $q_0\sim10^{14}$ W/cm^2. The degree of polarization of the second harmonic amounted to ~50 in energy. The change from p- to s-polarized heating radiation was effected by rotating the polarization plane of the infrared radiation with the aid of a $\lambda/2$ plate and simultaneous rotation of the KDP crystal through 90°. To separate the radiation at the 0.53 μm wavelength, an SZS-21 color filter was placed behind the KDP crystal. The energy flux density at the target at 1.06 μm wavelength did not exceed in this case 10^4 W/cm^2.

The experiments were performed with oblique (45°) incidence of s- and p-polarized radiation on a polyethylene, aluminum, or bismuth target. The radiation at the frequencies $\omega_0/2$ and $3\omega_0/2$ was observed simultaneously in the direction along the normal to the target plane. When the polarization of the harmonic radiation was investigated, a high-aperture polarizer was placed in the registration channel.

To register the laser-plasma emission spectra we used the monochromators MDR-2 ($\omega_0/2$ region) and MDR-3 ($3\omega_0/2$ region) (Fig. 1). The exit focal planes of the monochromators were made to coincide with the planes of the electron-optic image converter cameras (EDC) of type UMI-93. It must be noted that the large absorption of the radiation at the frequency $3\omega_0/2$ ($\lambda=0.35$ μm) in the photographic lenses made it impossible to use the standard input photoattachments customarily used in EOC. To carry out the spectral-temporal measurements the time-scan slit was located directly in front of the spectral slit of the monochromator. The spectral and temporal resolutions of the measurements depended principally on the type of chosen diffraction grating and on the order of its spectrum. In our experiments the spectral resolutions were ~2 Å and ~4–8 Å for the $3\omega_0/2$ and $\omega_0/2$ harmonics, and the temporal resolution was ~100 psec. The reference lines used for the determination of the shifts in the harmonic emission spectra were the 1.06 and 0.53 μm laser lines registered in each shot.

4. Figure 2 shows photomicrographs of the $3\omega_0/2$ harmonic spectra, obtained in the case of p-polarized pump radiation for three targets with different atomic numbers. The emission spectrum of the $3\omega_0/2$ harmonic has one component shifted towards the red relative to the value of $3\omega_0/2$; the shift increases with increasing atomic number of the target. Thus, the shift is ~10 Å for polyethylene, ~15 Å for aluminum, and ~27 Å for the bismuth target. The broadening of the red component hardly changes and amounts to 10–15 Å. The form of the spectrum of the $3\omega_0/2$ harmonic and its intensity are practically independent of the heating-radiation polarization. The emission of the $3\omega_0/2$ harmonic has strictly the laser polarization.

Similar photomicrographs for the $\omega_0/2$ harmonic are shown in Fig. 3. The spectrum has a two-component structure. The components are located on opposite sides of the exact value $2\lambda_0$. The distance between the components in-

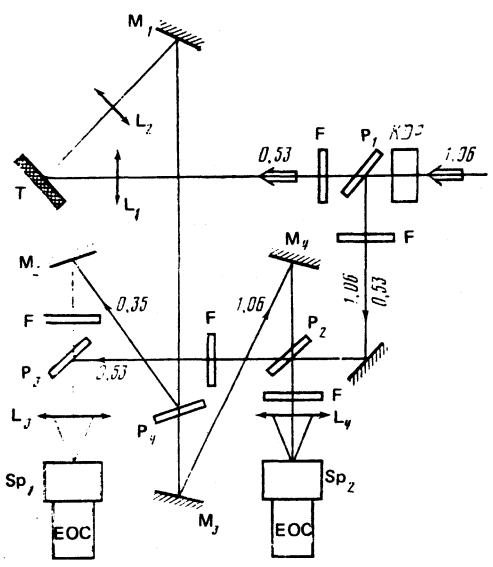

FIG. 1. Experimental setup. T) Target, M_1—M_4) mirrors, L1—L4) lenses, F) light filters, P1—P4) glass plastes, Sp_1, Sp_2) spectrographs, EOC) electron-optical camera.

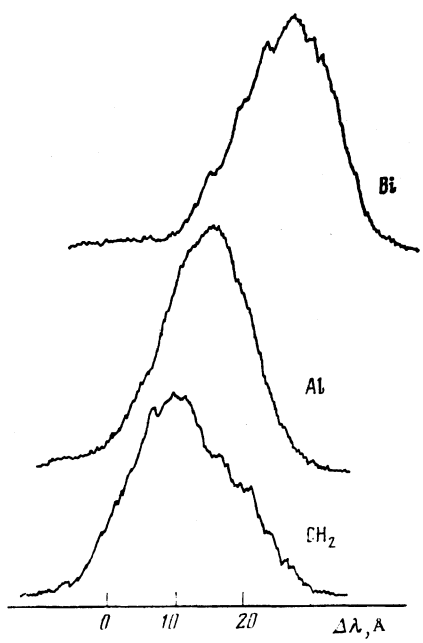

FIG. 2. Photomicrographs of emission spectra at frequency $3\omega_0/2$ for three targets.

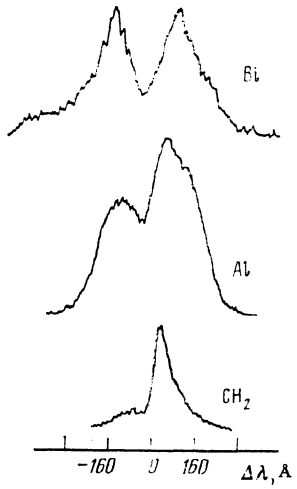

FIG. 3. Photomicrographs of emission spectra at frequency $\omega_0/2$ for three targets.

creases with the number Z of the target, and the intensities of the red and blue components become equalized. We note that the components are asymmetric about the value $2\lambda_0$. The blue component is shifted by a large amount for all the employed targets. For example, for an aluminum target $\Delta\lambda_{red} = 70$ Å and $\Delta\lambda_{blue} = 100$ Å. The shifts of the spectral components of the $\omega_0/2$ harmonic, their width, and their intensity, just as in the $3\omega_0/2$ case, are independent of the incident-radiation polarization. Spectrograms were obtained in two polarization planes of the laser radiation. In the latter case the intensity of the blue component exceeds that of the red (Fig. 4). It can be concluded from the results of the polarization measurements that the $\omega_0/2$ radiation is noticeably depolarized, with the depolarization of the blue component considerably stronger.

Figure 5 shows the following temporal spectrograms: a) of the radiation at frequency $\omega_0/2$; b) of the heating radiation and of the radiation at frequency $3\omega_0/2$. It can be seen that intense radiation of harmonics is present only in the first half of the laser pulse and pulsates noticeably with time, with a period $\tau \approx 300$ nsec. Both spectrograms were obtained in one shot for an aluminum target with p-polarized pumping. Similar results were obtained for polyethylene and bismuth targets, and it was observed that the duration of the harmonic

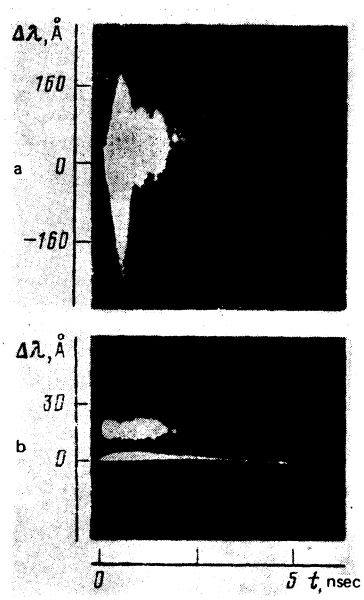

FIG. 5. Temporal spectrograms of the radiation at the frequency $\omega_0/2$ (a), $3\omega_0/2$ and the heating radiation (b). Aluminum target.

radiation decreases with increasing atomic number of the target (Fig. 6) and their intensity decreses substantially.

5. We begin the analysis of the experimental results with a discussion of the thresholds of the parametric instabilities. The minimum thresholds of the two-plasmon instability in SRS in the $n_c/4$ region coincide for a spatially homogeneous plasma and are determined by the electron-ion collisions (see, e.g., Ref. 15):

$$q_{0\,\mathrm{thr}} = 1.2 \cdot 10^{11}\, \bar{Z}^2/T_e^{\,3}\lambda_0^{\,4}\ \mathrm{W/cm^2}, \qquad (5.1)$$

where $\bar{Z}$ is the average ion charge, T_e is the electron temperature in keV, and λ_0 is the wavelength of the heating radiation in microns. In order for $q_{0\,\mathrm{thr}}$ not to exceed the mean value $q_0 \times 10^{14}$ W/cm^2 it is necessary that the electron temperature in the $n_c/4$ region be sufficiently high:

$$T_e \geqslant 0.25\, \bar{Z}^{2/3}\ \mathrm{keV}. \qquad (5.2)$$

For polyethylene ($\bar{Z} = 2.7$) this condition is satisfied at $T_e \gtrsim 0.5$ keV, for aluminum ($\bar{Z} = 10$) at $T_e \gtrsim 1.2$ keV, and for

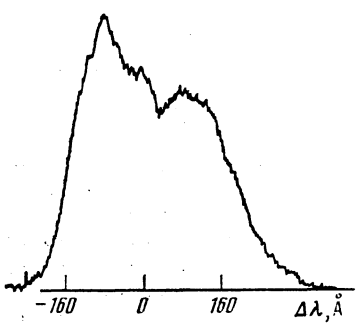

FIG. 4. Photomicrograph of emission spectrum at frequency $\omega_0/2$ for the component polarized perpendicular to the laser-radiation incident plane. Case of s-polarization, aluminum target.

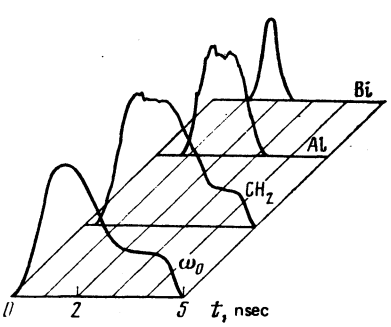

FIG. 6. Time microphotograms of heating radiation ω_0 and of the radiation at frequency $3\omega_0/2$ for three targets.

bismuth ($\bar{Z} \sim 30$–40) the threshold temperature is already 2.4–2.9 keV.

In an inhomogeneous plasma, the stability threshold is higher than (5.1). For two-plasmon instability, the influence of the inhomogeneity scale L on the thresholds begins to manifest itself at[16]

$$L/\lambda_0 < (\omega_0/4\nu_{ei})^2 (v_{Te}/c)^2 \approx 10^4\, T_e^4 \lambda_0^2/\bar{Z}^2, \qquad (5.3)$$

where v_{Te} is the electron thermal velocity, and ν_{ei} is the electron-ion collision frequency. For $T_e \approx 1$ keV, $\lambda_0 = 0.53\,\mu$m, and $Z = 10$ it follows from (5.3) that $L \lesssim 10\,\mu$m.

For the SRS process the influence of the inhomogeneity turns out to be stronger. According to Ref. 17, the threshold of the SRS instability increases ($q_{\text{thr}} \propto L^{-4/3}$) at

$$L/\lambda_0 < (\omega_0/4\nu_{ei})^{1/2} \approx 4 \cdot 10^4 T_e^{3/4} \lambda_0^{1/2}/\bar{Z}^{1/2}. \qquad (5.4)$$

From this, at the same values of the parameters T_e, λ_0, and $\bar{Z}$ we obtain $L < 200\,\mu$m.

The foregoing estimates show that the SRS threshold should be much higher than the threshold of two-plasmon decay, and is not reached in our experiments. Confirming this are also the half-integer harmonic spectra (see Figs. 2 and 3), which should be considerably more broadened under SRS conditions.[18]

6. We discuss now the harmonic-radiation spectra. It is known[7,19,20] that at normal incidence of the radiation on the target the spectrum of the $3\omega_0/2$ harmonic should have two components. Such a spectrum was observed earlier, in particular, also with our installation.[8] At oblique incidence of the pump wave the intensity ratio of the components depends on the observation direction. According to the theory,[12] when the observation is along the normal to the target, the blue component in the spectrum of the $3\omega_0/2$ harmonic should be suppressed. The spectrum of the $3\omega_0/2$ harmonic calculated for the experimental conditions in the plane-layered plasma approximation is shown in Fig. 7. Comparison of the experimental data (see Fig. 2) with Fig. 7 indicates a qualitative agreement between theory and experiment.

For the spectrum of the $3\omega_0/2$ to be distinguishable above the thermal level it is necessary that the convective gain $\varkappa$ of the plasma waves[12] exceed unity

$$\varkappa = {}^1/_{24}\pi (v_E^2/v_{Te}^2) k_0 L (1 - {}^4/_3 \sin^2\theta_0)^{-1/2} > 1. \qquad (6.1)$$

In Eq. (6.1), $v_E = eE_0/m\omega_0$ is the oscillatory velocity of the electron in pump field E_0, θ_0 is the angle of incidence of the pump wave on the plasma, and k_0 is its wave vector. From (6.1) at $q_0 = 10^{14}$ W/cm^2 and $T = 1$ keV we obtain the estimate $L \gtrsim 100\,\mu$m for the scale of the plasma density inhomogeneity in the $n_c/4$ region.

The shift of the line maximum ($\Delta\lambda_{1/2}$) relative to the exact value $2\lambda_0/3$ is connected with the electron temperature by a relation given in Ref. 12. For the irradiation and observation geometry used in the experiment we have

$$T_e = 400\, \Delta\lambda_{1/2}/\lambda_0 \text{ keV}. \qquad (6.2)$$

The corona temperatures determined from the red shift $\Delta\lambda_{3/2}$ of the spectrum of the $3\omega_0/2$ harmonic are shown in Table I. It can be seen that the temperature rises with increasing atomic number of the target material. On going from polyethylene to bismuth, T_e increases by approximately three times. We note that an increase of $\Delta\lambda_{3/2}$ with increasing atomic number of the target material was observed also in earlier experiments[5,6] with radiation at the wavelength 1.06 μm. Thus, for example, in Ref. 5 an analogous increase of $\Delta\lambda_{3/2}$ by a factor of three was observed on going from a deuterium to a copper target.

The $3\omega_0/2$ harmonic radiation is connected with Raman scattering of the heating radiation by the Langmuir waves. According to the theoretical premises,[12,19] the polarization of the harmonic should coincide in this case with the polarization of the heating radiation. This agrees well enough with the experimental results.

The Raman-scattering cross section is proportional to the energy density of the Langmuir waves. When the $3\omega_0/2$ harmonic is observed along the direction of the plasma-density inhomogeneity, the component transverse to the gradient of the vector of the Langmuir waves from which the scattering takes place is equal in absolute value, by virtue of the momentum conservation law ($\mathbf{k}_{l\perp} = \mathbf{k}_{3/2\perp} - \mathbf{k}_{0\perp}$), to the transverse component $k_{l\perp} = k_{0\perp} = 2^{-1/2}\omega_0/c$ of the pump-wave vector. Since the growth rate of the two-plasmon instability is proportional to the scalar product of the pump-wave polarization vector and to Langmuir wave vector, the excitation of the Langmuir waves that participate in the Raman scattering is connected only with the p-component of the pump wave. In addition, the p-polarized pump wave excites plasmons that propagate almost along the density gradient. The spectrum of the $3\omega_0/2$ harmonic can contain then wave with large frequency shifts.[12,21,22] Therefore the spectrum of the $3\omega_0/2$ harmonic at a p-polarized pump wave should have according to the theory a larger intensity and width than in

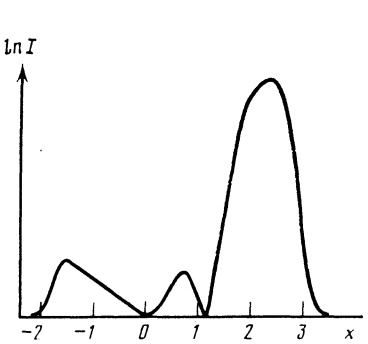

FIG. 7. Theoretical spectrum of the $3\omega_0/2$ harmonic in the case of p-polarization of the pump wave. The abscissas are the values of $x = (c^2/v_{Te}^2)(\Delta\lambda/\lambda_0)$.

TABLE I. Determination of the temperature in the $n_c/4$ region from the spectra of the $3\omega_0/2$ harmonic [see Eq. (6.1)].

Material	CH_2		Al	Bi
	s	p		
$\Delta\lambda_{3/2}$, Å	9	10	15	27
T_e, keV	0.7	0.8	1.2	2.1
Relative increment of the temperature	1		1.35	2.8

the case of s-polarization. Experiments revealed no such regularities.

7. The radiation at the frequency $\omega_0/2$ is also connected with Langmuir turbulence in the $n_c/4$ region, but the coincidence of the harmonic-generation region with the region of its critical density complicates somewhat the description of the radiation process. Namely, besides the Raman scattering, as in the case of the $3\omega_0/2$ harmonic, the $\omega_0/2$ harmonic radiation can be connected also with linear transformation of the Langmuir waves into transverse ones (see Ref. 12). The strong $\omega_0/2$-radiation depolarization observed in experiments points to an important role of linear transformation as a mechanism for $\omega_0/2$ radiation. At the same time, linear transformation alone cannot explain fully the aggregate of the experimental facts. By virtue of the momentum conservation law in two plasmon decay, only Langmuir waves with frequencies $\omega_0/2$ propagate in the direction of increasing plasma density.[12] Since only waves that travel into the interior of the plasma can undergo linear transformation, it follows that if the Raman scattering were neglected there would remain in spectrum of the $\omega_0/2$ harmonic only the blue component. Consequently the red component in the $\omega_0/2$ spectrum must be attributed to Raman scattering. The difference between the physical characters of the appearance of the red and blue components is confirmed by results of polarization measurements (see Figs. 3 and 4), from which it follows that the red component is more weakly depolarized than the blue one. The comparable intensities of the blue and red components of the $\omega_0/2$ harmonic for a bismuth target indicate that the probabilities of the two processes are approximately the same in this case.

It can be seen from Fig. 3 that the intensity of the blue component in the spectrum of the $\omega_0/2$ harmonic, for light-element targets, is lower than the intensity of the red one. Bearing in mind the observed increase of temperature with increase of the atomic number (see Table I), it can be concluded that the efficiency of linear transformation of longitudinal waves into transverse ones increases with rising temperature. According to the theory,[12] the coefficient of linear transformation of Langmuir waves into the $\omega_0/2$ harmonic increase $\propto T_e^{3/2}$.

Since the red component in the spectrum of the $\omega_0/2$ harmonic is connected with Raman scattering, we can again use the results of the theory[12] and speak of a proportionality of the shift of the maximum ($\Delta\lambda_{1/2}$) of the red component relative to the exact value $2\lambda_0$ and of the electron temperature in the $n_c/4$ region. For the geometry of irradiation and observation used in the experiment we have[12]

$$T_e = 110\,\Delta\lambda_{1/2}/\lambda_0 \text{ keV}. \qquad (7.1)$$

The values of T_e calculated from the shift of the red component in the spectrum of the $\omega_0/2$ harmonic are given in Table II. From a comparison of Tables I and II it can be seen that the values of T_e obtained from the spectrum of the $\omega_0/2$ harmonic are somewhat higher than those that follow from the $3\omega_0/2$ spectrum. In our opinion, this difference is connected with the insufficient inaccuracy of Eq. (7.1) because the region of generation of the $\omega_0/2$ harmonic coincides with its critical region.

TABLE II. Determination of the temperature in the $n_c/4$ region from the shift of the red component in the spectrum of the $\omega_0/2$ harmonic [see Eq. (7.1)]

Material	CH_2	Al	Bi
$\Delta\lambda_{1/2}$, Å	45	100	130
T_e, keV	0.9	2.0	2.7
Relative temperature increment	1	1.9	2.6

At the same time, the observed tendency of T_e to increase with increasing atomic number of the material is also seen from Table II. The relative changes of the temperatures on going from polyethylene to aluminum and bismuth are approximately equal in Tables I and II. This fact confirms the direct proportionality of $\Delta\lambda_{1/2}$ and T_e in Eq. (7.1).

Intense radiation of the $\omega_0/2$ and $3\omega_0/2$ harmonics exists only during the first half of the pulse for targets of aluminum and bismuth (see Figs. 5 and 6). This may be due to the form of the laser pulse, which has in the first half (Fig. 6) a maximum power approximately double the average.

In addition, the use of the data of Table I in Eq. (5.1) indicates that at $q_0 = 10^{14}$ W/cm^2 the dissipative threshold for polyethylene has been exceeded by approximately three times; for aluminum this flux value is the threshold. Therefore the instability-excitation time, and hence also the radiation time and the intensity of the harmonics should be somewhat smaller for the aluminum than for the polyethylene target. The threshold flux for bismuth is $q_0 = 2\times 10^{14}$ W/cm^2. This means that the excitation of the two-plasmon instability is possible only near the maximum of the laser pulse, as is indeed seen in Fig. 6.

8. The foregoing analysis of the experimental data allows us to conclude that at a laser radiation wavelength 0.53 μm and at an energy flux 10^{14} W/cm^2 a two-plasmon parametric instability is excited even on targets with large atomic numbers.

Many of the observed characteristics of the half-integer harmonics (angular directivity of the radiation, form of the spectrum, etc.) are satisfactorily explained within the framework of the existing theoretical concepts (Refs. 12, 19–22). At the same time, a number of the observed effects have not found a satisfactory theoretical explanations. The causes of the shift of the center of the doublet of the $\omega_0/2$ harmonic relative to the exact value $2\lambda_0$ are unknown; the reason why the characteristics of the harmonics do not depend on the pump polarization is not clear.

One of the most important results of the present study is observation of a growth of the corona temperature (in the $n_c/4$ region) with increasing atomic number of the target material. A similar dependence was observed earlier[23] in an investigation of soft x rays from a laser plasma. Such a $T_e(Z)$ dependence cannot be explained within the framework of classical theory of radiation absorption and heat transfer, but it can nevertheless be understood by starting from the assumption that a collision-free heat transfer takes place and manifests itself in a limitation of the electron thermal conductivity. The suppression of the thermal conductivity of a

laser plasma is an experimentally established fact.[24–29]

Writing down the electron heat flux in the conventional form $n_c T_e v_{Te} f$, we obtain from its equality to the absorbed laser-radiation flux the customarily used expression for the coefficient f:

$$f=\alpha q_0/n_c T_e v_{Te}, \tag{8.1}$$

where α is the absorption coefficient. Inasmuch as in the experiments performed the absorption coefficient amounted to $\alpha \sim 1$ and was practically independent of the target material, the observed increase of the temperature with increasing atomic number of the target material is evidence of enhancement of the effect of limitation of the thermal conductivity on going from light to heavy elements. In accordance with Table I we obtain $f_{CH_2}:f_{Al}:f_{Bi} = 0.2:0.1:0.04$.

One of the possible mechanisms responsible for the limitation on the thermal conductivity is ion-sound turbulence. It has been shown within the framework of the theory[30] that the restriction on the thermal conductivity is larger than larger ZT_e/T_i, the increase of the latter facilitating the excitation of the ion-sound turbulence. For example, in the case of a Maxwellian distribution of the ions we obtain for the coefficient f (Ref. 30)

$$f\approx {}^1/_6 (Z/A)^{1/2}(1+1.8\delta) n_e/n_c, \tag{8.2}$$

where the parameter δ characterizes the rate of dissipation of the energy of the ion-sound waves on account of the Čerenkov effect on the ions:

$$\delta=43\left[\frac{A}{Z}\left(\frac{ZT_e}{T_i}\right)^3 \exp\left(-\frac{ZT_e}{T_i}-3\right)\right]^{1/2} \tag{8.3}$$

(A is the atomic weight of the ions). The quantity n_e in (8.2) should be taken to mean the characteristic electron-density value corresponding to the heating-radiation absorption region. It is clear that if the usual inverse-bremsstrahlung introduces an appreciable contribution to the absorption, this region shifts with increasing Z towards the rarefied corona. According to (8.2) and (8.3), in the case of a weak dependence of the ratio T_e/T_i on the target material the increase of Z is accompanied by a decrease of both δ and the ratio n_e/n_c, i.e., it leads to a decrease of f. Thus, on the basis of (8.2) and (8.3) one can speak of a qualitative correspondence of the established fact, that the temperature increases with increasing Z, with the result of the theory of anomalous transport due to the development of the ion-sound turbulence,[30] since it follows from (8.1) that at one and the same value of the heating-radiation flux a higher electron temperature corresponds to smaller values of f. A quantitative comparison of (8.2) with the estimate that follows for f from (8.1), using in the latter the experimentally obtained values of T_e, is in the general case difficult, since there is no information on the ion temperature that determines the parameter δ. At the same time, in the case of a bismuth target ($Z\sim 40$), when it can be assumed that $\delta \ll 1$, we obtain from (8.2) $f\approx 0.07 n_e/n_c$. This estimate agrees with the one that follows from (8.1) at $n_e \sim 0.5 n_c$, thus pointing to a substantial absorption of the heating radiation in the subcritical-density region.

[1]V. V. Aleksandrov, N. G. Koval'skiĭ, and V. P. Silin, Zh. Eksp. Teor. Fiz. **79**, 850 (1980) [Sov. Phys. JETP **52**, 432 (1980)].
[2]J. Soures, L. M. Goldman and M. J. Lubin, Nuclear Fusion **13**, 829 (1973).
[3]J. L. Bobin, M. Decroisette, B. Meyer, and Y. Vittel, Phys. Rev. Lett. **30**, 594 (1973).
[4]Ping Lee, D. V. Giovanelli, R. P. Godwin, and G. M. McCall, Appl. Phys. Lett. **24**, 409 (1974).
[5]M. C. Pant, K. Eidmann, P. Sachsenmaier, and R. Sigel, Opt. Commun. **16**, 396 (1976).
[6]V. V. Aleksandrov, V. D. Vikharev, V. P. Zotov, N. G. Koval'skiĭ, and M. I. Pergament, Pis'ma Zh. Eksp. Teor. Fiz. **24**, 551 (1976) [JETP Lett. **24**, 508 (1976)].
[7]A. I. Avrov, V. Yu. Bychenkov, O. N. Krokhin, *et al.*, Pis'ma Zh. Eksp. Teor. Fiz. **24**, 293 (1976) [JETP Lett. **24**, 262 (1976)]. Zh. Eksp. Teor. Fiz. **72**, 970 (1977) [Sov. Phys. JETP **45**, 507 (1977)].
[8]L. M. Gorbunov, Yu. S. Kas'yanov, V. V. Korobkin, A. N. Polyanichev, and A. P. Shevel'ko, FIAN Preprint No. 126, 1979.
[9]J. Elazar, W. T. Toner, and E. R. Wooding, Plasma Phys. **23**, 813 (1981).
[10]A. V. Kil'pio, A. A. Malyutin, and P. P. Pashinin, Pis'ma Zh. Eksp. Teor. Fiz. **32**, 520 (1980) [JETP Lett. **32**, 499 (1980)].
[11]E. McGoldrick and S. M. L. Sim, Opt. Commun. **40**, 433 (1982).
[12]V. Yu. Bychenkov, A. A. Zozulya, V. P. Silin, and V. T. Tikhonchuk, FIAN Preprint No. 136, 1981. V. Ju. Bychenkov, A. A. Zozulya, V. P. Silin, and V. T. Tikhonchuk, Beitr. Plasmaphys. **23**, 1 (1983).
[13]V. P. Silin, Parametricheskoe vozdeĭstvie izlucheniya bol'shoĭ moshchnosti na plazmu (Parametric Action of High-Power Radiation on a Plasma), Nauka, 1973, §26.
[14]V. L. Artsimovich, L. M. Gorbunov, Yu. S. Kas'yanov, and V. V. Korobkin, Zh. Eksp. Teor. Fiz. **80**, 1859 (1981) [Sov. Phys. JETP **53**, 963 (1981)].
[15]Yu. V. Afanas'ev, N. G. Basov, O. N. Krokhin, *et al.*, Interaction of High-Power Laser Radiation with a Plasma, Itogi nauki i tekhniki, ser. Radiofizika 17, Chaps VI and VII, VINITI, 1978.
[16]E. Z. Gusakov, A. D. Piliya, and V. I. Fedorov, Fiz. Plazmy **3**, 1328 (1977) [Sov. J. Plasma Phys. **3**, 739 (1977)].
[17]J. F. Drake and Y. C. Lee, Phys. Rev. Lett. **31**, 11979 (1973). V. P. Silin and A. N. Starodub, Zh. Eksp. Teor. Fiz. **67**, 2110 (1974) [Sov. Phys. JETP **40**, 1047 (1975)].
[18]L. M. Gorbunov, V. P. Silin, and V. T. Tikhonchuk, Fiz. Plazmy **6**, 663 (1977) [Sov. J. Plasma Phys. **6**, 364 (1977)].
[19]V. Yu. Bychenkov, V. P. Silin, and V. T. Tikhonchuk, Fiz. Plazmy **3**, 1314 (1977) [Sov. J. Plasma Phys. **3**, 730 (1977)].
[20]E. Z. Gusakov, Pis'ma Zh. Tekh. Fiz. **3**, 1219 (1977) [Sov. Tech. Phys. Lett. **3**, 504 (1977)].
[21]V. P. Silin, Kratk. soobshch. Fiz. FIAN No. 10, 35 (1979).
[22]A. A. Zozulya and V. P. Silin, Kratk. Soobshch. Fiz. FIAN No. 1, 49 (1981).
[23]V. V. Blazhenkov, A. N. Kurkin, L. P. Kotenko, *et al.*, Zh. Eksp. Teor. Fiz. **78**, 1386 (1980) [Sov. Phys. JETP **51**, 697 (1980)].
[24]R. C. Malone and R. L. McCrory, Phys. Rev. Lett. **34**, 721 (1975).
[25]J. S. Pearlman and J. P. Ahthes, *ibid.* **27**, 581 (1975) [*sic*!].
[26]P. M. Campbell, R. R. Johnson, F. J. Mayer, L. V. Poners, and D. C. Slater, Phys. Rev. Lett. **39**, 274 (1977).
[27]R. Benattar, C. Popovics, R. Sigel, and J. Virmont, Phys. Rev. Lett. **42**, 766 (1979).
[28]M. H. Key, Phil. Trans. Roy. Soc. London **A298**, 351 (1980).
[29]T. Jabe, K. Mima, and K. Yoshikawa, Preprint ILE 8003P, Osaka Univ., 1980.
[30]V. Yu. Bychenkov and V. P. Silin, Zh. Eksp. Teor. Fiz. **82**, 1886 (1982) [Sov. Phys. JETP **55**, 1086 (1982)]. V. Yu. Bychenkov, O. M. Gradov, and V. P. Silin, Zh. Eksp. Teor. Fiz. **83**, 2170 (1982) [Sov. Phys. JETP **56**, 1257 (1982)].

Translated by J. G. Adashko